

Indoor Positioning System Infrastructure Based on Triangulation Method through Visible Light Communication

Apnan Juanda¹, Willy Anugrah Cahyadi², Angga Rusdinar³, Denny Darlis⁴

^{1,2,3}Electrical Engineering, School of Electrical Engineering, Telkom University, Bandung, Indonesia
⁴Telecommunication Technology, School of Applied Science, Telkom University, Bandung, Indonesia

¹apnanjuanda@student.telkomuniversity.ac.id, ²waczze@telkomuniversity.ac.id,

³anggarusdinar@telkomuniversity.co.id, ⁴dennydarlis@telkomuniversity.ac.id

Accepted on 11 September 2021

Approved on 14 December 2021

Abstract— Autonomous mobile robots are widely used in industry to help human's work, but the concept has a weakness, that is robot still does not know its position in a room so it can not detect whether the robot has been at destination point. The technology commonly used to determine the position of objects is the Global Positioning System (GPS). However, GPS does not detect objects that are indoors. Previous research used Wi-Fi as a reference for designing an indoor positioning system, but the system could not determine the position in detail because Wi-Fi could only detect object zones. Based on these problems, this research will propose the infrastructure prototype design of an indoor positioning system based on Visible Light Communication (VLC). The main focus of this research is designing a VLC transmitter and receiver system, estimating the distance between the receiver and transmitter based on the received signal strength, and estimating the receiver's position using the triangulation method based on a minimum of 3 distance estimates. The estimating distance system get average accuracy is 76.47%. The estimated accuracy of the x-coordinate position has the best accuracy is 77.05% and the y-coordinate estimate has the best accuracy is 86.54%.

Index Terms— Indoor Positioning System; LED Driver; Log Normal Shadowing; Received Signal Strength (RSS); Triangulation; Visible Light Communication (VLC)

I. INTRODUCTION

Remotely Operated Underwater Vehicle (ROV) is a submersible robotic systems, used to examine various underwater characteristics and controlled by operators from shore[1]. With complex, dangerous and limited areas urgently explored, there is an urgent need for an underwater machine that can replace humans to complete underwater detection. ROV were developed to perform resource exploration tasks in the ocean[2]. The applications of ROV are widely diverse, such as the oil and gas industry, discovery, aquaculture, marine biology, and military purpose [3][4][5][6].

Numerous of ROV designs are assembled around or inside cubic structured frame along with a buoyant on top body. The robotic vehicle utilized umbilical data cable as electrical cable and controlled by operator positioned on surface vessel.

The heavier tools are settled down on lowest possible position to keep the point of center buoyancy is higher than center of gravity, thus adequate stability is obtained. Sufficient stability of ROV meant ROV has capability to withstand against in disturbance for instance moment of rolling and pitch in longitudinal and lateral axis. Steady hydraulic rods suited of lifting and carrying particular equipment for specific purpose and placed in the fore along with cameras and lights.

Underwater ROVs are generally divided categories based on size, weight, capacity, or performance. Two common design of ROV which widely use are: the ROV Micro-Class with weigh not higher than 3 kg, are used especially in narrow area where a diver might not be capable to enter. And the ROV Mini-Class that weigh about 15 kg are also used as a diver alternative, Inspection-Class are typically rugged ROVs for commercial or industrial use, data acquisition and observation ROVs, Light weight duty category has generally no more than 50 hp on propulsion, While Heavy duty type has less than 220 hp with the ability to capability lift at least two handlers and work at depths up to 3500 m, and Trenching & Burial work class is the largest with more than 200 hp propulsion, with the ability to take a cable, put down sleds and working at depths until 6000 m in several cases[7][8][9][10]. The ROV design and construction is a robust solution to encounter the various require of an ROV to be used in wide implementations, it is compact, handy to use and inexpensive, and allow for confined space exploration. The main form of the body is designed to encounter the particular utilization needs. Commonly, almost ROV attached by torpedo form and an hydrodynamic main body was used at high-speeds[11]. Another type is the torpedo-less form, worked mainly in remote control

vehicles (ROVs) that are often worked for shorter period of time purpose or the assessment of other large subsea areas like huge ice floe or water-dams[12]. Toward to emphasize the performance in water resistance, Computational Fluid Dynamics (CFD), drives valuable part in Unmanned vehicle design. Nowadays, CFD approach has been widely applied in underwater vehicle design, as it can simulate the fluid flow field around the bodies and to find out with comprehend the physics of fluid flow phenomenon. CFD captured the flow field such as vortex in very small to major scales which is hard to obtain through field experiments.

CFD methods enable to predict and diagnostic technique for identifying the cause of particular problem in physic phenomena. The latest CFD approaches provide wealth data generated emphasize to visualize the implication of the result requires considerable skill. Due to this CFD become as an integral part of the design process.

From the economic cost, numerical simulation can deliver result within sufficiently short time span in the design process, thus optimization design can be detailed in addition to addressing this issue during the design process. Numeric simulation is considered low cost analysis hence became early stage to understanding along side with experimental test which can be over cost and intensive time.

In this project, the CFD analysis assists in investigate and demonstrate variable model for the hull body form based on initial prototype [13]. In this research, a design of Mini-ROV is developed especially the principal of body device in each element and electric parts is embedded. Furthermore, the hydrodynamic parameter and analysis was provided based on CFD simulation.

II. METHODS

The experimental method was used in this study, where a series of experiments were directly conducted by theoretical studies. The overall block diagram of the system built is shown in Fig. 1.

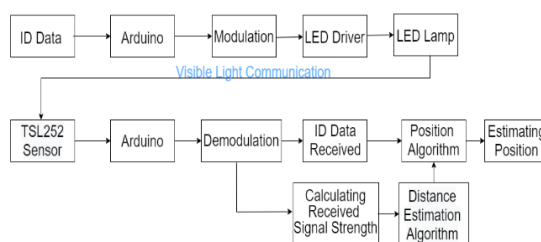


Fig. 1. Block Diagram System

The explanation in Fig. 1 is as follows: first Data ID will be initialized on Arduino, next it converted into ASCII data and will generate binary code that will be sent with serial communication UART (Universal Asynchronous Receiver-Transmitter). The modulation

process is carried out, namely the process of converting the information into the carrier signal in the form of LED light. LED Driver is used as a switching circuit that converts the UART signal into LED's light, on the receiver side, the TSL252 sensor works to receive the light intensity and then performs a demodulation process so that the ID data is retrieved, next estimating distance process is based on the received signal strength and estimating position based on the triangulation method.

The prototype that will be made consists of 4 lamps with a height is 80 cm from the floor, between lamps given a distance is 40 cm and the height of the photodetector sensor to the lamp is 65 cm. Based on the existing block diagram, the first step is to initialize the ID data which is the letters of the alphabet a, b, c, d. This ID will be identity and coordinate(x, y) information of each lamp [11]. Next, Arduino Uno which as a microcontroller transmitter will convert data ID into UART serial format and forward it to LED Driver MOSFET IRF520 module. Data will be sent via visible light communication using modulation on-off keying [12].

The receiver device will use the TSL252 sensor to receive the light intensity and convert it into electrical pulses [13]. It is a combination of photodiode and transimpedance amplifier. Photodiode and transimpedance amplifier function to convert light intensity into voltage. The receiver circuit cable configuration is done by connecting the sensor ground pin to the Arduino ground pin, the VCC sensor pin to the 5V Arduino pin, the sensor OUT pin is connected to the Arduino RX pin. The system uses a grid separate and 4 TSL252 sensors to avoid incoming data collisions and cause data bits to be interference and can not be converted to ID data. Identify the incoming signal from which lamp based on the ID data received by the receiver system. Calculating the power of each received signal use log normal shadowing equation to estimate the distance receiver to transmitter. In this research, the process of measuring the distance between the transmitter and the receiver is based on the Received Signal Strength (RSS) method.

Several methods are conceptually capable to solve the problems. Examples of the most common methods are Time Different of Arrival (TDOA) and RSS. Based on TDOA the distance calculates by utilizing the required time to send data from transmitter to receiver so the time will be comparable with the traveled distance. Whereas the RSS used the current signal at the receiver where if the distance between transmitter and receiver is short that received signal will get more power. Because the speed of lights is very high, applying the TDOA method to design a prototype is difficult to calculate how much time it takes for transmitter to send data to receiver at each test point. Therefore an easier method to apply in this research is the RSS method which used the signal strength and

partition between sensors so each sensor only receives one signal from a specific transmitter and avoids interference of signals from other transmitters.

Based on the RSS method when the received power is greater, the distance between transmitter and receiver is getting closer, and vice versa [14]. The log normal shadowing model is used to calculate the estimated distance by knowing in advance the power value at the reference point, the power at the test point and the pathloss exponent value. The power at the reference point is the power when the receiver is directly under a lamp or transmitter. The pathloss exponent value is a coefficient that indicates a reduction in transmit power when the transmitter sends data until the data is successfully received at the receiver. Next step, estimating receiver position using distance estimation data and triangulation method [15].

The triangulation method can be used to determine the position of an object only by referring to the distance of three existing points. The way to do this is to draw a straight line that connects two points whose distance can be measured directly. The distance between the two points is carefully measured. Then the angle formed by a line connecting one point to the object to be determined is the distance from the line connecting the two points is measured. Then the angle between the line connecting the second point with the object with the line connecting the two points is also measured. Based on the information of two angle values and the distance of three points, the object distance can be calculated.

The design of system will be divided into 3 parts, namely: transmitter device, receiver device, and then design of estimated distance and position. This is an illustration of the overall positioning system that will be created.

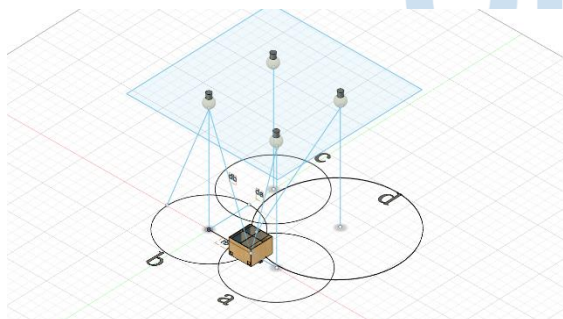


Fig. 2. Illustration Overall System Design

Explanation of Fig. 2 is prototype will be designed to use 4 LED lights as part of the transmitter device that will send ID data, then the illustration of the brown box is the object whose position will be estimated, in which a receiver sensor will be installed to receive data and based on the data and the intensity of the light it will be estimated the distance and position of the object to the transmitter, then the circle in the picture shows the range of data reception

A. Transmitter Device

The transmitter hardware design consists of a 20 Watt 12 VDC LED lamp, LED Driver IRF520, 12 VDC power supply, and an Arduino Uno microcontroller.

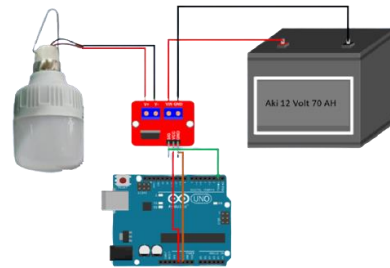


Fig. 3. Wiring Diagram of Transmitter

Next, the software design of the transmitter is shown in flowchart Fig. 3. It explains the sequence of commands when Arduino sends ID data via UART serial communication format and then proceeds to MOSFET IRF520 module to modulate the intensity of LED light.

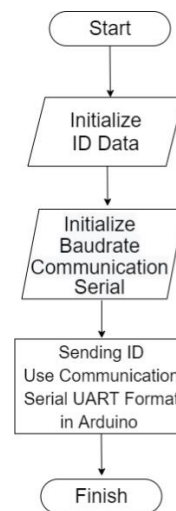


Fig. 4. Flowchart of Transmitter

The explanation in Fig. 4 is a process of sending data by the transmitter. First, the data will be initialized on the Arduino then the baudrate communication will be set for UART format serial communication. The data in the form of an alphabet will be converted into an ASCII code in the form of a binary code, then the process is continued to the LED driver for data adjust the blinking of the lamp to match the transmitted binary data.

B. Receiver Device

The receiver hardware design consists of 4 sets of TSL252 sensors and Arduino Nano, Arduino Mega, and LCD Display 16x2.

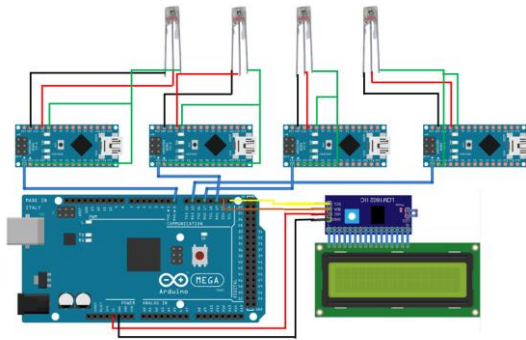


Fig. 5. Wiring Diagram of Receiver

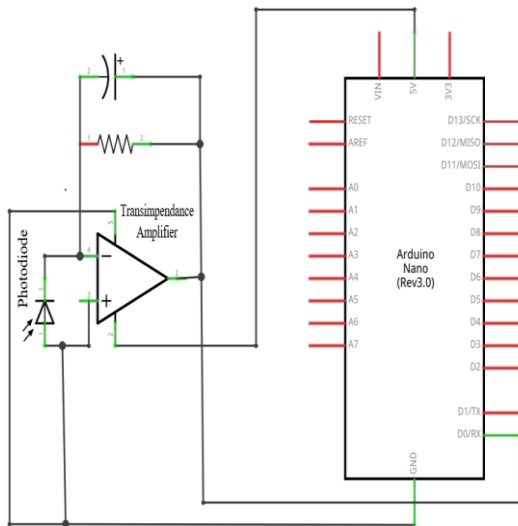


Fig. 6. Schematic of TSL252 Sensor

The TSL252 sensor consists of a photodiode and a transimpedance amplifier function to convert intensity light into voltage or electrical pulses in UART serial format to be translated into ID data. Next, Arduino will calculate the Received Strength for each signal.

The software design of receiver is shown in flowchart Fig. 6. Because the received signal must know 2 types of data, the first stage of the receiver flow diagram is initializing analog pins to read voltage data and the baudrate initialization used must be the same as the transmitter baudrate.

Furthermore, if there is already a data ID in the serial buffer, if there is, then proceed to the data reading process, otherwise the system will wait for the data to be available again. After the ID data is obtained, the process of converting the ADC value to the voltage value is continued. The last process on the VLC Receiver device is the packaging of ID and voltage data which will later be used as input data in the distance estimation process.

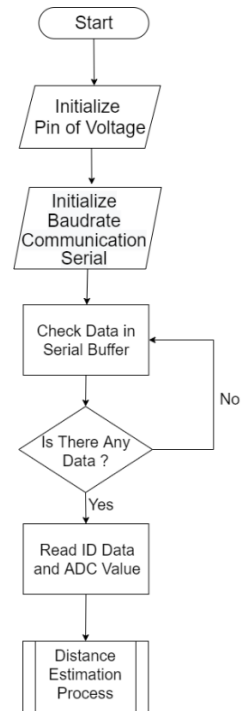


Fig. 7. Flowchart of Receiver

Explanation of Fig. 7 is a process that occurs in the receiver. first, initialize the output pin TSL252 sensor then initialize the baudrate used and must be the same as the baudrate on the transmitter, and then proceed with asynchronous serial communication, if there is data in the serial buffer then, the system detect ID data and ADC value then proceed to the process of estimating the distance from the receiver to the transmitter based on the data ID data and received signal strength.

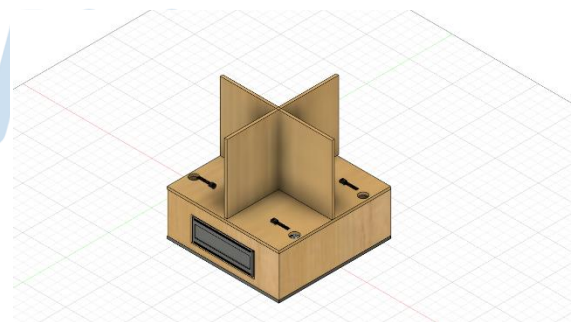


Fig. 8. Mounting and Separation Sensor Design

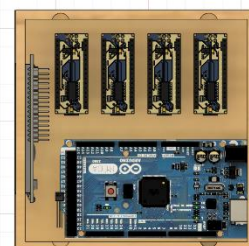


Fig. 9. Components Laying Design

The explanation for Fig. 8 and 9 are the illustration of the object to be estimated position where the TSL252 sensor has been placed to read the data, Arduino to process the data, and a 16x2 LCD to display the estimated position of the object coordinate. The Separator is used so that each sensor only focuses on receiving 1 ID data and avoids the influence of other ID data signals.

C. Design of Estimated Distance and Position Algorithm

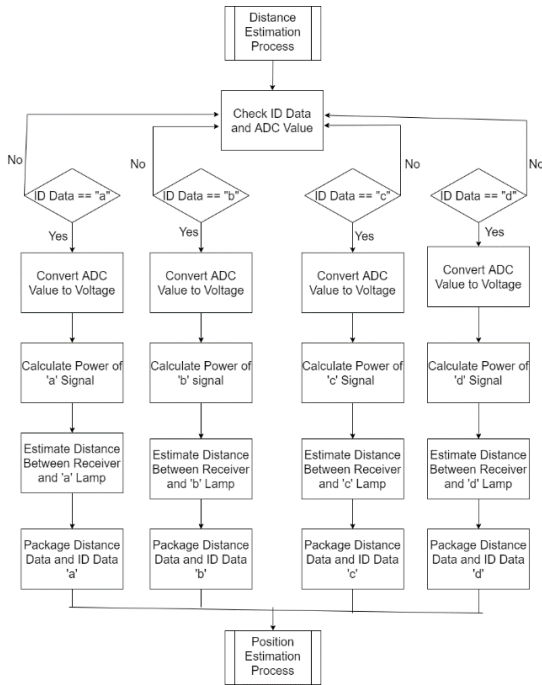


Fig. 10. Flowchart of Estimated Distance

When the ID data is received by the receiver, the system will simultaneously read the signal voltage and calculate the power. Furthermore, the receiving power of each signal will be calculated then the system will use the log normal shadowing equation to estimate the direct distance (d) of the receiver to the lamp that becomes transmitter.

$$Prx = P_0 - 10.n.\log\left(\frac{d}{d_0}\right) \quad (1)$$

After that, by using the Pythagoras theorem, the radius distance will be obtained.

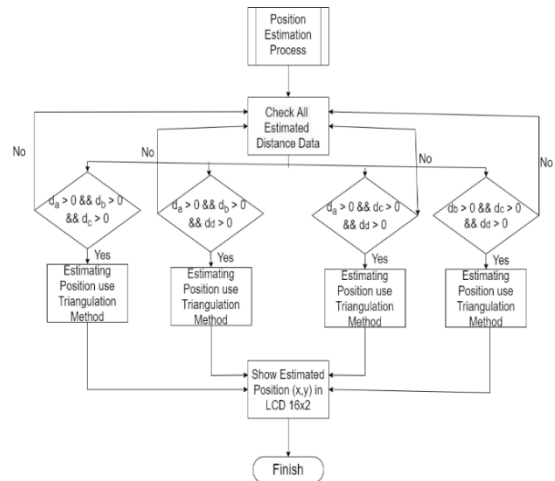


Fig. 11. Flowchart of Estimated Position

The first step in the positioning system flow chart is to check all data on the estimated distance from the receiver to the transmitter. Then check the data based on 4 conditions that have been determined. If one of the conditions is true then the position estimation can be done using the triangulation method.

This is an equation to find the coordinate of an object's position based on estimated distance data and the triangulation method. This equation requires a distance estimate of at least 3 data

$$\begin{bmatrix} x \\ y \end{bmatrix} = \begin{bmatrix} 2(x_2 - x_1) & 2(y_2 - y_1) \\ 2(x_3 - x_1) & 2(y_3 - y_1) \end{bmatrix}^{-1} \begin{bmatrix} r_1^2 - r_2^2 - (x_1^2 + y_1^2) - (x_2^2 + y_2^2) \\ r_1^2 - r_3^2 - (x_1^2 + y_1^2) - (x_3^2 + y_3^2) \end{bmatrix} \quad (2)$$

This is the prototype of the designed system:



Fig. 12. Prototype

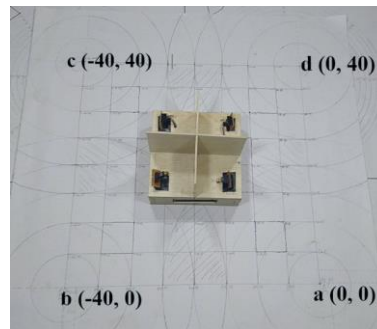


Fig. 13. Reference Coordinates

III. RESULT AND DISCUSSION

The testing in this research is divided into 3 parts: testing of send and receive data through Visible Light Communication (VLC), estimating the distance between receiver and transmitter based on Received Signal Strength (RSS), and estimating the position of object based on triangulation method.

A. Analysis of Sending Data

The analysis is done by observing the transmit signal that appears on the oscilloscope screen, started with connecting the oscilloscope signal cable to the Arduino TX pin as a transmitter and the oscilloscope ground cable to the Arduino ground pin.

a) Signal of ID "a"

The transmit signal is converted into binary data so that ID "a" becomes 0110001, then the oscilloscope will read the signal in the Least Significant Bit (LSB), which is reading data start from the binary data row which has the smallest value, the signal displayed is 0100001101. The number 0 at the beginning start bit and the last 1 indicates the stop bit

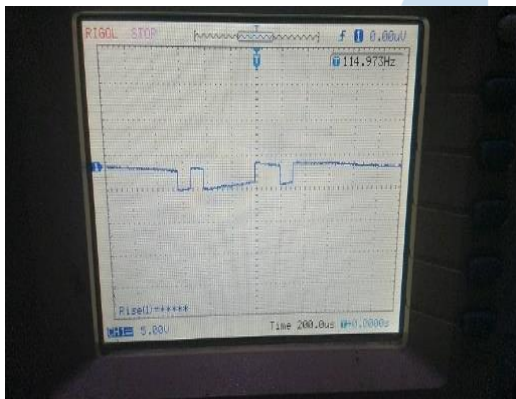


Fig. 14. Signal Form of ID a

b) Signal of ID "b"

The transmit signal is converted to binary data becomes 01100010, on the oscilloscope the signal that appears is 0010001101.

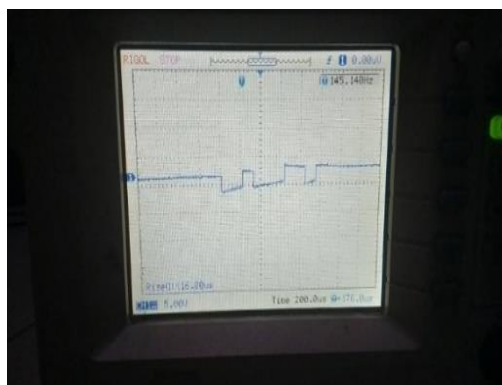


Fig. 15. Signal Form of ID b

c) Signal of ID "c"

The transmit signal is converted to binary data becomes 01100011, on the oscilloscope the signal that appears is 0110001101.

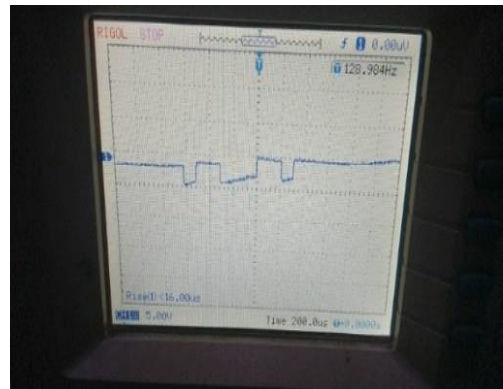


Fig. 16. Signal Form of ID c

d) Signal of ID "d"

The transmit signal is converted to binary data becomes 01100100, on the oscilloscope the signal that appears is 0001001101.

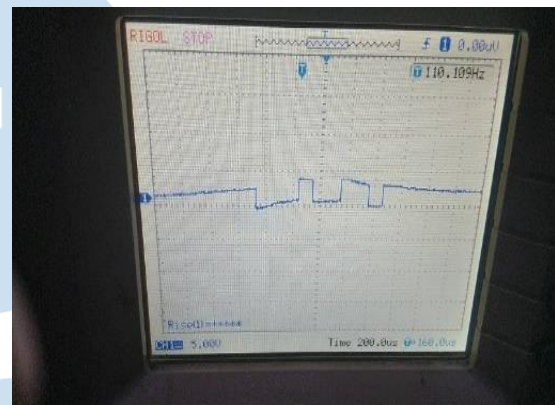


Fig. 17. Signal Form of ID d

B. Analysis of Light Intensity to Radius Distance

This analysis is to determine the value of the light intensity transmitter lamp when the TSL252 sensor can receive ID data at the farthest radius distance from the transmitter. The measurement process uses lux meter HS1010.

TABLE I. LIGHT INTENSITY TO RADIUS DISTANCE

ID of Lamp	Distance Radius (cm)	Ligth Intensity (Lux)
a	0	362
	5	336
	10	326
	15	366
	20	329
	25	164
b	0	362
	5	347
	10	326
	15	290
	20	214
	25	132
c	0	387

	5	348
	10	340
	15	330
	20	282
	25	219
d	0	371
	5	318
	10	311
	15	290
	20	242
	25	172

Based on Table 1, the signal can be received with a maximum radius distance is 25 cm and the required light intensity in the range of 150 - 370 lux.

C. Analysis of Received Signal

This Analysis is carried out at several points representing positions in center and extreme positions. Center Positions were tested at (-10, 15); (-30, 15); (-30, 25); (-10, 25) while extreme positions were tested at (-10, 30) and (-10, 10). Extreme positions are coordinate position x, y which tend to be very close to one lamp or transmitter but far enough from the other lamp. The purpose of this test is to find out what ID data is received by the receiver device and then it was processed as input to estimate the distance between receiver and transmitter.

TABLE II. RECEIVED SIGNAL AT COORDINATE POSITION TEST

Coordinate Position	Received ID	Signal Strength (mW)	Description
(-10, 15)	a	2.897	Center Position
	d	2.78	
	b	2.781	
(-30,15)	b	2.775	Center Position
	c	2.861	
	a	2.777	
(-30, 25)	c	2.89	Center Position
	b	2.76	
	d	2.72	
(-10, 25)	d	2.98	Center Position
	a	2.8	
	c	2.82	
(-10, 30)	a	2.76	Extreme Position
	c	2.57	
	d	3.08	
(-10,10)	a	2.91	Extreme Position
	d	2.97	
	b	2.85	

Distance Estimation System is done by first calculating the pathloss exponent value of each lamp based on the received signal strength and the log normal shadowing equation. The suitability of the pathloss exponential value is tested by comparing the estimated radius distance based on the system with the real radius distance.

D. Analysis of Estimated Distance between Receiver and Transmitter

a) Calculating Pathloss Exponent Value

Distance Estimation System is carried out by calculating the pathloss exponent value of each lamp based on the received signal strength and the log normal shadowing equation. The suitability of the pathloss exponential value is tested by comparing the estimated radius distance based on the system with the real radius distance.

TABLE III. PATHLOSS EXPONENT VALUE

ID	Radius Distance (cm)	Prx (mW)	d (cm)	n	Average n
a	0	3.066	65	0	3.188
	5	2.9805	65.192	6.674	
	10	2.841	65.765	4.430	
	15	2.797	66.708	2.388	
	20	2.5845	68.007	2.451	
b	0	3.1665	65	0	3.607
	5	3.0535	65.192	8.820	
	10	2.9135	65.765	4.981	
	15	2.8825	66.708	2.521	
	20	2.8295	68.007	1.716	
c	0	3.049	65	0	3.322
	5	2.9245	65.192	9.718	
	10	2.8885	65.765	3.160	
	15	2.786	66.708	2.334	
	20	2.7745	68.007	1.397	
d	0	3.094	65	0	3.276
	5	2.983	65.192	8.664	
	10	2.882	65.765	4.173	
	15	2.8455	66.708	2.206	
	20	2.8315	68.007	1.336	

The pathloss exponential value contained in table III is based on calculations using the log normal shadowing equation.

$$Prx = P_0 - 10.n.\log\left(\frac{d}{d_0}\right) \quad (3)$$

It requires some parameters, namely:

P₀ : Received Signal Strength at reference point when the radius distance is 0 cm (receiver is right below the lamp as transmitter).

P_{rx} : Received Signal Strength at position test.

n : pathloss exponential value.

d : direct distance between receiver, and transmitter.

d₀ : direct distance between receiver and transmitter when radius distance is 0 cm.

After being measured and calculated the results obtained are as follows:

d_{0a} = d_{0b} = d_{0c} = d_{0d} = 65 cm, P_{0a} = 3.066 mW, P_{0b} = 3.1665 mW, P_{0c} = 3.049 mW, P_{0d} = 3.094 mW. For the value of d and the value of n as represented in Table III. The following graph shows the radius distance will decrease signal strength

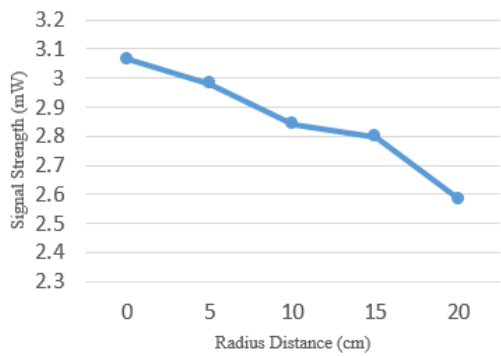


Fig. 18. Radius Distance to "a" Signal Strength Graph

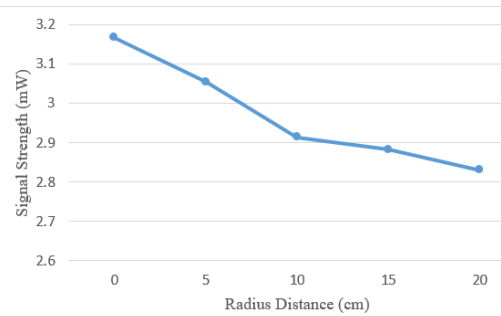


Fig. 19. Radius Distance to "b" Signal Strength Graph

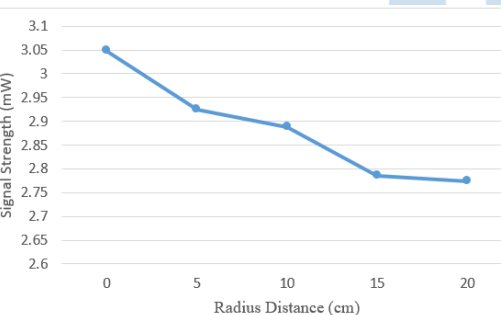


Fig. 20. Radius Distance to "c" Signal Strength Graph

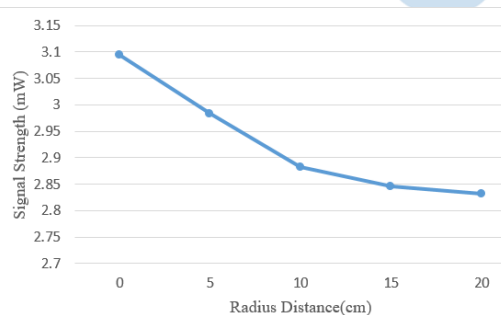


Fig. 21. Radius Distance to "d" Signal Strength Graph

b) Analysis of Estimated Distance Radius with Pathloss Exponent Value

Testing the pathloss exponent value is done by estimating the direct distance (d) using the log normal shadowing equation and then comparing it with the real direct distance (d). Furthermore, the distance d is used

to calculate the value of radius distance (r), next it was compared with the actual radius distance r.

TABLE IV. ESTIMATED DIRECT DISTANCE

ID	Prx (mW)	d estimated (cm)	d real (cm)
a	3.066	65	65
	2.981	65.403	65.192
	2.841	66.065	65.765
	2.797	66.275	66.708
	2.585	67.3	68.007
b	3.167	65	65
	3.054	65.471	65.192
	2.914	66.058	65.765
	2.883	66.189	66.708
	2.83	66.413	68.007
c	3.049	65	65
	2.925	65.563	65.192
	2.889	65.727	65.765
	2.786	66.196	66.708
	2.775	66.249	68.007
d	3.094	65	65
	2.983	65.509	65.192
	2.882	65.976	65.765
	2.846	66.145	66.708
	2.832	66.21	68.007

TABLE V. ESTIMATED & ACCURACY RADIUS DISTANCE

r estimated (cm)	r real (cm)	Error (%)	Accuracy (%)	Average Accuracy (%)
0	0	0	100	76.47
7.246	5	44.91	55.088	
11.81	10	18.14	81.865	
12.94	15	13.75	86.252	
17.44	20	12.78	87.219	
0	0	0	100	
7.835	5	56.7	43.299	
11.78	10	17.76	82.237	
12.49	15	16.74	83.262	
13.63	20	31.86	68.141	
0	0	0	100	
8.576	5	71.53	28.473	
9.75	10	2.501	97.499	
12.53	15	16.5	83.502	
12.8	20	35.99	64.007	
0	0	0	100	
8.151	5	63.02	36.975	
11.31	10	13.05	86.948	
12.26	15	18.3	81.704	
12.6	20	36.99	63.011	

The explanation of Table V is showed radius distance data based on estimates and real conditions, after calculated the average accuracy reaches 76.47%

E. Analysis of Estimated Position Based on Triangulation Method

This test uses several coordinate positions that represent positions in center and extreme position such as at the ends of the lamp

a) Center Position area

TABLE VI. ESTIMATED IN CENTER POSITION AREA

Coordinate Test	Received ID	Prx (mW)	d estimated(cm)
-----------------	-------------	----------	-----------------

(-10, 15)	a	2.897	65.798
	d	2.78	67.306
	b	2.781	66.619
(-30,15)	b	2.775	66.645
	c	2.861	65.853
	a	2.777	66.371
(-30, 25)	c	2.89	65.72
	b	2.76	66.709
	d	2.72	67.59
(-10, 25)	d	2.98	66.366
	a	2.8	66.261
	c	2.82	66.04

The explanation Table VI is showed the test results when the object is positioned in the center of area, then ID and received signal strength are noted on the receiver side next using equation 1 in the method section to obtain the value of d which is the distance between the transmitter and the receiver.

TABLE VII. COORDINATE ESTIMATED IN CENTER POSITION AREA

r estimated (cm)	Coordinate x	Coordinate y
10.218	-18.641	17.49145
17.467		
14.599		
14.715	-19.5446	21.31197
10.562		
13.42		
9.7037	-23.1161	21.63587
15.001		
18.532		
13.398	-20.5402	19.82483
12.864		
11.674		

The explanation of Table VII showed estimated radius distance data from each transmitter to the receiver. Then it is used to find the estimated coordinate position based on equation 2 on method section

b) Extreme Position area

TABLE VIII. d ESTIMATED IN EXTREME POSITION AREA

Coordinate Test	Received ID	Prx (mW)	d Estimated (cm)
(-10, 30)	a	2.76	66.452
	c	2.57	67.194
	d	3.08	65.902
(-10,10)	a	2.91	65.736
	d	2.97	66.413
	b	2.85	66.326

The explanation Table VIII is showed the test results when the object is positioned in an extreme area, then ID and received signal strength are noted on the receiver side next using equation 1 in the method section to obtain the value of d which is the distance between the transmitter and the receiver.

TABLE IX. COORDINATE ESTIMATED IN EXTREME POSITION AREA

r Estimated (cm)	Coordinate x	Coordinate y
13.817	-17.8491	20.91135
17.032		
10.863		
9.8121	-19.026	18.88234
13.627		
13.198		

The explanation of Table IX showed estimated radius distance data from each transmitter to the receiver. Then it is used to find the estimated coordinate position based on equation 2 in the method section.

c) Estimated Coordinate x Position Accuracy

Based on data in table VII and IX, it can be calculated the accuracy of coordinate x is shown in table X.

TABLE X. ACCURACY COORDINATE X

Coordinate Test	Estimated Coordinate x	Accuracy x (%)	Average Accuracy x (%)
(-10, 15)	-18.641	13.59	30.27
(-30,15)	-19.5446	65.14867	
(-30, 25)	-23.1161	77.05367	
(-10, 25)	-20.5402	-5.402	
(-10, 30)	-17.8491	21.509	

(-10,10)	-19.026	9.74	

d) Estimated Coordinate y Position Accuracy

TABLE XI. ACCURACY COORDINATE Y

Coordinate Test	Estimated Coordinate y	Accuracy y (%)	Average Accuracy y (%)
(-10, 15)	17.491446	83.39036	64.67
(-30,15)	21.311972	57.92019	
(-30, 25)	21.635873	86.54349	
(-10, 25)	19.824829	79.29932	
(-10, 30)	20.911346	69.70449	
(-10,10)	18.882339	11.17661	

The explanation of Table X and XI is showed a comparison of coordinate data (x, y) based on estimates and real conditions, next the percentage of accuracy is calculated.

Coordinate Test 1 (-10, 15)
 Estimated Coordinate 1 (-18.641, 17.491)



Fig. 22. Coordinate 1

Coordinate Test 2 (-30, 15)
 Estimated Coordinate 2 (-19.545, 21.312)



Fig. 23. Coordinate 2

Coordinate Test 3 (-30, 25)
 Estimated Coordinate 3 (-23.116, 21.636)



Fig. 24. Coordinate 3

Coordinate Test 4 (-10, 25)
 Estimated Coordinate 4 (-20.540, 19.825)



Fig. 25. Coordinate 4

Coordinate Test 5 (-10, 30)
 Estimated Coordinate 5 (-17.849, 20.911)

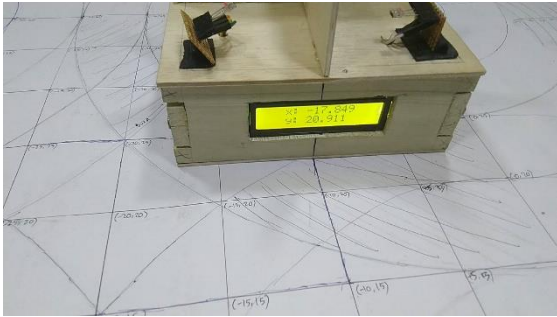


Fig. 26. Coordinate 5

Coordinate Test 6 (-10, 10)
Estimated Coordinate 6 (-19.026, 18.882)



Fig. 27. Coordinate 6

F. Analysis of Environment Condition

In this research, the lamp used is limited to 20 watts, because based on testing the transmitter device with specifications of the lamp is good enough to send ID data signal but if the lights used are brighter or dimmer the next research it can be added to the design of the Automatic Gain Controlled (AGC) circuit which is a circuit able regulating the gain in a system and controlling it automatically. This prototype is expected to be able to detect the robot when it reaches the destination point but indeed with all limitations. The focus of this work is only on making the infrastructure of the system which includes sensors, microcontrollers, entering formulas into the programming code and the sequence of processes carried out from receiving data by sensors. To be processed using equations if in a real condition prototype must add some additional parts such as filter circuit and optical lens in the receiver device.

IV. CONCLUSIONS

A. Research's Results

The Transceiver device of Visible Light Communication (VLC) succeeded in sending and receiving data in the form of alphabets letters which consists of "a" until "d" with a maximum radius distance is 25 cm and a maximum angle for data transmission is 21.056° .

The design process of positioning estimation system can be solved through several stages are as follows: first step, the receiver of VLC can receive data

from the three closest transmitters when tested in the center area and the extreme area. Second step, the distance estimation system between receiver and transmitter can be done with an average accuracy is 76.47%. Furthermore, based on ID and distance estimation data, a positioning estimation system can be carried out and the system get the best accuracy of x-coordinate estimation is 77.05% and the best accuracy of y-coordinate estimation is 86.54%.

Then if it is calculated, the average accuracy of x-coordinate is 30.27% and y-coordinate is 64.67%. The average accuracy is not so good because the data received at a certain test point does not obtain data with maximum accuracy because there are still deficiencies in the positioning of the sensor.

B. Future Work

- 1) Designing device interfaces can display estimated position data.
- 2) Two-way communication can be implemented by combining with infrared (IR) communication.
- 3) Design of filter circuits and optical lenses on the receiver so that noise can be minimized and the signal becomes more focused to receive

REFERENCES

- [1] I. P. D. Wibawa, A. Rafif, A. Rusdinar, "Design of Tracking System Based on Sensor Fusion (Encoder and Accelerometer) for AGV Position Monitoring," e-Proceeding of Engineering, vol. 6, no. 2, pp. 1-8, 2019, ISSN : 2355-9365
- [2] M. A. Khairul, I. P. Pangaribuan, R. Nugraha, "Food Delivery System Using Augmented Guided Vehicle (AGV) Line Follower Completed Barcode", e-Proceeding of Engineering, vol. 7, no. 2, pp. 3091-3105, 2020, ISSN : 2355-9365
- [3] W. Jatmiko¹, M. S. Alvissalim², A. Febrian³, and dan D. R.Y.S⁴, "Autonomous Robot Localization Method Using The Adoption of Heuristic Searching and Pruning Algorithm for Map Development in Search-And-Safe Case", Jurnal Ilmu Komputer dan Informasi, vol. 2, pp. 114-123, ISSN 1979 - 0732
- [4] F. T. Ashegaf, B. A. D. Naipospos, B. B. Bimantoro, "Electric Wheelchair with User Health Monitoring System, Location and Accident Detection Based on IoT", ejournal3.undip.ac.id, vol. 8, no. 2, pp. 119-127, 2019, e-ISSN:2685-0206
- [5] H. Liu, and J. L. Houshang Darabi, Pat Banerjee, "Survey of Wireless Indoor Positioning Techniques and Systems", IEEE TRANSACTIONS ON SYSTEMS, MAN, AND CYBERNETICS, vol. 37, no. 6, 2007.
- [6] D. P. Yudha, B. I. Hasbi, and R. H. Sukarna, "Indoor Positioning System Based on Fingerprinting Received Signal Strength (RSS) WIFI With K-Nearest Neighbor (K-NN) Algorithm", ILKOM Jurnal Ilmiah, vol. 10, no. 3, pp. 274-283, 2018, e-ISSN 2548-7779 p-ISSN 2087-1716
- [7] S. Afifah, R. A. Priramadhi, D. Darlis, "Transceiver On Lighting for Warehouse Navigation System Based On Visible Light Communication", Annual Applied Science and Engineering Conference, 2018
- [8] A. P. Ardi, I. S. Aulia, R. A. Priramadhi, and D. Darlis, "VLC-Based Car-to-Car Communication," Jurnal Elektronika dan Telekomunikasi, vol. 20, no. 1, pp. 16-22, Aug. 2020. doi: 10.14203/jet.v20.16-22
- [9] C. Xuefen, D. Jing, L. Shuangxing, S. Wenxiao, W. Chunyue, W. Lang, "The Research of Indoor Positioning Based on Visible Light Communication", China Communications, vol. 12, no. 8, pp. 85-92, 2015

- [10] M. M. Rahmwati, N. M. Adriansyah, B. Pamukti, "Impact of The Number of Light Emitting Diode (LED) Towards The Accuracy in Indoor Positioning System Based on Visible Light Communication (VLC)", e-Proceeding of Engineering, vol. 7, no. 2, pp. 3758–3765, 2020, ISSN : 2355-9365
- [11] R. Irawan, Ilhamsyah, Y. Brianorman, "Application of Short Message Encrytion and Decription Using Android-Based Knapsack Algorithm", Jurnal Coding Sistem Komputer Untan, vol. 3, no. 3, pp. 57–66, 2015, ISSN 2338-493X
- [12] Z. Ghassemlooy, S. Arnon, M. Uysal, Z. Xu, and J. Cheng, "Emerging optical wireless communications- advances and challenges," IEEE journal on selected areas in communications, vol. 33, no. 9, pp. 1738–1749, 2015.
- [13] T. Instrument, "LMx58-N Low-Power, Dual-Operational Amplifiers," Texas Instrument, 2014.
- [14] S. M. Sheikh, H. M. Asif, K. Raahemifar, and F. Al-Turjman, "Time Difference of Arrival Based Indoor Positioning System Using Visible Light Communication," IEEE Access, vol. 9, pp. 52113–52124, 2021.
- [15] W. Dharmawan and A. Kumianto, "Increasing Accuracy of RSSI Distance Estimation with Normal Log Normal Using Kalman Filter Method on Bluetooth Low Energy", Seminar Nasional Sains dan Teknologi 2016 Fakultas Teknik Universitas Muhammadiyah Jakarta, no. 22, pp. 1–5, 2016, e-ISSN : 2460 – 8416 p- ISSN : 2407 – 1846

